

THEORETICAL STUDY OF ENVISAT'S THERMAL IR LIGHT CURVES

C. Mercier⁽¹⁾, U. Tricoli^{*(1)}, E. Coiro⁽¹⁾, Y. Abautret⁽¹⁾, J.-F. Sauvage⁽¹⁾, and C. Petit⁽²⁾

⁽¹⁾DOTA, ONERA, 13330 Salon-de-Provence, France

⁽²⁾DOTA, ONERA, Université Paris-Saclay, 92320 Châtillon, France

*Email: ugo.tricoli@onera.fr

ABSTRACT

The fast increase of abandoned objects in space is becoming a dangerous threat preventing to launch new missions or to guarantee operational standards. Hence, it is crucial to follow and track space debris. Optical techniques offer cheap alternative relatively to their radar counterpart. Especially, when low resolution imaging is exploited to get fast object tracking from telescopes. Nevertheless, optical tracking in the visible spectrum suffers the limitation related to the Sun illumination conditions in order to get enough light to detect the object when it lies in the shadow of the Earth. We therefore study the possibilities offered by thermal infrared optical detection in the LWIR band in order to be able to ensure the tracking in the absence of direct solar light. Hence, we developed a 3D thermal model for space objects. This model is based on COMSOL [7] and exports temperature maps to feed the emitted radiance calculation for all the parts lying on the space-pointing external surface of a satellite. We used the SIRIUS code [6] for the evaluation of the optical signature of space objects in the thermal bands (taking into account the Sun and Earth radiative contributions and the emitted thermal flux of the satellite). This tool, based on GPU implementation, generates hyperspectral images highly spectrally and spatially resolved. In particular we focus on a theoretical study of the tracking of ENVISAT as maybe the most known European debris. We then evaluate light curves in the visible and in the LWIR bands in order to study the gain of information carried out by infrared telescope observations. Until now, very few studies have been performed in the IR range focusing especially on near earth objects [17] but these relevant results lead to believe that it is an interesting way of investigations also for debris and satellites [32]. We will in particular study the part of the scenario where ENVISAT lies in the shadow of the Earth and consider the effects of the Earth emission on the LWIR light curves. The reflectivity of ENVISAT is modeled by the Spectral Bidirectional Reflectance Distribution Function (sBRDF) for each material with physical modelling of geometry wrinkling for the MLI. Emissivity spectra are also taken into account for the different materials. The radiative environment is composed by the Sun and the Earth. Finally, the orbit is calculated through the use of TLE files. To summarize, the paper will study theoretically the gain of information

related to a spatially non-resolved optical detection of a satellite from a ground telescope in the thermal infrared bands in order to understand the type of information that can be obtained in the IR bands and to track the satellite when it lies in the shadow of the Earth. The key quantity that will be considered is the IR light curve and its dependence on the Earth emissivity map and atmosphere, the thermal/optical materials on ENVISAT, the transient between the solar lighting and shadow phases and the (possible) thermal effect of electronics onboard the satellite.

Keywords: RSO, light curve, simulation, satellite, hyperspectral, IR, signature.

1. INTRODUCTION

The rapid increase of resident space objects (RSO) is calling for new fast and effective methods to identify, track and detect them. The vast majority of the remote sensing data comes from radar and optical imaging. The first ones [21] are mainly used to detect targets in low Earth orbit (LEO) while optics allows to access higher orbits. However, ground-based space telescopes of GEO objects can only provide very low spatial resolution making the use of light curves the main source of information (being the diameter of the observing instrument insufficient to spatially resolve the targeted object). Optical modeling of space objects is an interesting way to understand light curves and to develop inversion techniques to obtain important information as the mass, the optical properties, the shape and the attitude to mention a few. For example, Hejduk et al. [16] introduced a model based on the approximation of the observed object by a Lambertian sphere or with diffuse and specular reflective properties. Although the attitude of the object was not considered, the method makes it possible to reproduce in an overall quite satisfactory manner the magnitude of objects such as GEO satellites and space debris [29], or satellite mega constellations [24]. To address the case of observations of GEO satellites at large phase angles, Coignon [5] has complicated this model by modeling the shape with a sphere and a rectangle for the solar panels, in order to take into account the reflection of the Earth on the satellite. However, these simple models are no longer suf-

ficient when resolved detection is considered and/or to analyze the spectral information of the RSO. More recently, some studies were dedicated to understand RSO taking into account spatial resolution through imaging techniques both experimentally and theoretically. For example, a high-performance ground telescope with atmospheric turbulence correction by adaptive optics can provide low-resolution images of large LEO satellites such as ENVISAT [27]. On the simulation side there has been now many studies dedicated to extract satellite information from spatially resolved simulation (thus calculating images of the target satellites) as in [10] and to understand light curve features. Other interesting studies in this direction are related to the PROXOR code [15], the VISIONE code [28] and the DIRSIG code [32] more focused on the evaluation of the RSO signature from detailed spatial and spectral information for imaging. Other optical models of resolved objects are described in the literature, but present limitations. Y. Wang et al. [34] and H. Wang et al. [33] for example used simplified rendering techniques linked to real-time constraints, which do not allow complex reflections to be represented. In addition, global illumination rendering methods seem the most realistic to date. AirbusGroup [9] has developed a comprehensive tool based on this technique to generate images mainly intended for satellite classification and to address the approach and landing phases. Other techniques as space based observation means to detect RSO can generate highly resolved images to get object signatures [23]. Interestingly some of them start to observe in the thermal infrared around 10 μm as in [17, 25]. Recently, the possibility to observe in the thermal infrared spectrum is becoming of interest and remarkably through observations with ground telescope [30, 26]. Our study here aims to evaluate the gain of information that can be obtained by expanding non-resolved ground telescope observations into the thermal infrared bands in combination with the traditional visible band.

2. THE MODEL

In order to perform simulations of a satellite thermal IR signature many complicated variables of a space scenario must be considered. First of all the kinematics of the Sun (the source), the Earth (the main thermal emitter) and the satellite need to be taken into account. For that task, the code SIRIUS (ultra spectral interactive image simulator) developed at ONERA was used [18, 19, 31, 6]. This type of modeling belongs to the high spatial and spectral resolution imaging simulations as in [15, 32, 28]. Secondly, the thermal forcing of the Sun and the Earth plus the radiative/conductive contributions of the satellite itself need to be taken into account. We thus developed a satellite thermal model based on the COMSOL spacecraft thermal analysis [7] to get temperature maps of a satellite. Temperature maps along with the geometry of the satellite are used to evaluate the thermal emission of the object in the LWIR band. At last, all the radiative contributions (solar absorption, reflection, thermal emission) are calculated with SIRIUS and propagated through the atmo-

sphere to a detector (modeled as a simple camera through its aperture and the number of pixels of the collected image) to simulate the image that can be collected from an observer (here we restricted to a ground telescope type of observation even if space detection can be simulated too [31]). To evaluate the light curve we then calculated a series of images for the time interval of interest and averaged the radiance per pixel on every image (for the visible [380,780] nm and LWIR [8,12] μm bands).

2.1. The ultra spectral image simulator for space objects SIRIUS

The physics-based ray-tracing rendering engine we developed, SIRIUS ([18, 19, 31, 6]), is able to provide radiometrically accurate and physically correct hyperspectral images of satellites over time taking into account the complexity of space scenarios. The model simulates passive multidimensional optical imaging (from single-band to hyperspectral) from the visible to the thermal infrared band of the electromagnetic spectrum (from 380 nm to 14 μm). The code has the capability to simulate images of different satellites with high spatial and spectral resolution required for space-based satellite observations and ground-based telescope measurements. SIRIUS uses 3D satellite models in Wavefront OBJ format. Complex creased geometries as the multi layer insulation (MLI) can also be treated. The radiation coming from the Sun, reflected and thermally emitted by the Earth and its atmosphere is considered to calculate the specific intensity arriving at each pixel of the detector modeled as a camera with a tunable field of view (FOV). The thermal radiation which is emitted by the satellite is also considered for calculations in the LWIR band. The surface properties assigned to the geometry are those of the corresponding constituent materials i.e. bidirectional reflectance distribution function (BRDF) for accurate radiometric modeling and emissivity/ absorption coefficient (plus the thermal properties). Different BRDF models that are common in the literature as a pure specular or a lambertian reflector can be used in addition to a model for specular reflection with lobes. Trajectories of the observer and of the target should be given in CIC or TLE formats even if a fixed configuration can also be used. The attitude of the observed satellite (and of the observer if required) are also taken into account. The radiative contribution of the Earth atmosphere is also calculated with the ONERA radiative transfer code MATISSE [22] which is especially important for ground-based observation to get correct transmissions for every band. In addition, the effect of the Point Spread Function (PSF) of the instrument or atmospheric turbulence (for an observer on the ground or in the atmosphere) on image generation is also treated [3] through convolution product. Image resolution up to 5000x5000 pixels and spectral resolution up to 2000 bands can be achieved due to the parallel implementation of the ray-tracing algorithm on the graphic card (GPU). Finally, all the parameters can be initialized with the help of a graphic user interface which also allows for a quicklook visualization of the target satellite

as seen by the detector, trajectories visualization and material identification on the geometry of the satellite [31].

2.2. Thermal model

We want to analyze the thermal signature of a satellite (in this particular case ENVISAT), being observable even when the satellite is not under direct sunlight. In order to estimate the ENVISAT signature in the LWIR, we need to know its surface temperature. To do this, we developed a finite element thermal model using COMSOL Multiphysics and in particular the OTL Module [14]. Our model uses a simplified ENVISAT geometry we have generated, as knowledge of small spatial scales is not relevant for low resolution passive optical detection considered here (plus the randomization of reflected directions due to diffuse thermal emission). COMSOL has a physics based adaptive mesh functionality (in this case refining the mesh for the heat equation), and a sensitivity and validation study has been carried out through comparison with ESATAN [12] (for a simplified simple geometry as a cube corresponding to a cubesat).

The COMSOL spacecraft thermal analysis model uses two physics modules. First, the Heat Transfer In Solids which solves the heat equation:

$$\rho C_p \left(\frac{\partial T}{\partial t} + \mathbf{u} \cdot \nabla T \right) + \nabla \cdot \mathbf{q} = Q + Q_{ted} \quad (1)$$

$$\mathbf{q} = k \nabla T$$

with ρ the mass, C_p the specific heat capacity at constant pressure, \mathbf{u} the velocity vector, \mathbf{q} the conductive heat flux, Q the heat source, Q_{ted} the thermo-elastic damping, k the thermal conductivity and T the temperature [14]. Second, the Orbital Thermal Loads with the following equations:

$$\begin{aligned} J_i &= \varepsilon_i e_b(T) FEP_i(T) + \rho_{d,i} G_i \\ G_i &= G_{m,i} + G_{amb,i} + G_{ext,i} \\ G_{amb,i} &= F_{amb,i} \varepsilon_{amb} e_b(T_{amb}) FEP_i(T_{amb}) \\ e_b(T) &= n^2 \sigma T^4 \\ FEP_i(T) &= \frac{15}{\pi^4} \int_{C_2/(\lambda_i T)}^{C_2/(\lambda_{i-1} T)} \frac{x^3}{1-e^{-x}} dx \end{aligned} \quad (2)$$

with J the surface radiosity, ε the emissivity, e_b the beam orientation, FEP the fractional emissive power, G_m the mutual surface irradiation, G the surface irradiation, G_{amb} the ambient irradiation, G_{ext} the external irradiation, F_{amb} the ambient view factor, n the refractive index, σ the Stefan-Boltzmann constant, and $C_2 = hc/k_b$ [14]. Globally the thermal model takes into account a large number of parameters such as the thermal properties of materials (heat capacity, thermal conductivity, mass density) and optical properties (absorption and emission coefficients). It also takes into account volume properties like an internal heat source and the complex surface geometries such as the MLI which is modeled by a thin layer with its thermal and optical properties [13, 35]. Finally it takes into account the satellite's environment, such as the IR radiation from the Earth, with its non-homogeneous surface distribution, the Earth albedo map,

the radiation going to outer space and the Sun radiation. These radiative contributions and optical properties (absorption/emission) are spectrally divided in two bands, a solar band $\lambda \in [0; 2.5] \mu m$ and an IR environmental band $\lambda \in]2.5; +\infty[\mu m$. All these parameters were chosen for ENVISAT from [11] (with an internal heat source of 6.5kW). In order to take into account the satellite's orbit, we started with a TLE file at a date close to the desired time for simulation and ran a python code using Astropy and SGP-4 routine [2, 36] to generate all the parameters for an elliptical orbit at the desired dates such as Inclination (i), Right ascension of the ascending node (Ω), Eccentricity (e), Argument of perigee (ω), True anomaly (ν) and half major axis (a). To take into account the satellite's attitude, we used an estimation of the satellite's initial attitude, its angular velocities and its axis of rotation obtained in [21] by laser ranging and SAR measurements. We then calculated the attitude over time for the temporal window of interest. For thermal stabilization, our model calculates the four previous orbits before the temporal window of interest.

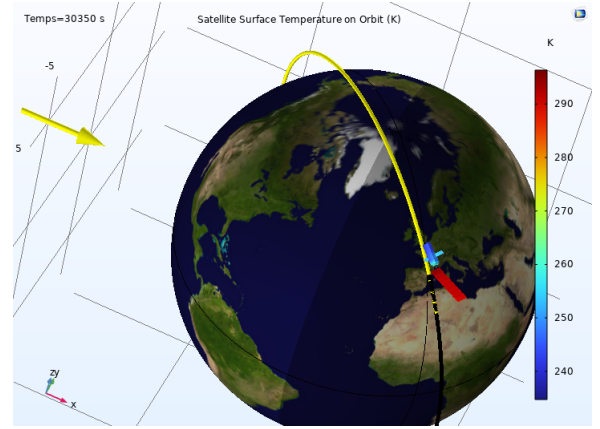


Figure 1. Example of the surface temperature on orbit calculated with COMSOL for ENVISAT on the day 2016-09-21T20-33-00.

Our thermal model provides surface temperature maps over time for each facet of the mesh. For integration purposes into the rendering tool SIRIUS, we averaged spatially the temperatures over each material defined in the geometry file. We considered three different materials for ENVISAT: The solar array, the MLI and the metal parts such as the satellite body and the radar antenna. These temperatures per material are formatted into a single file that can be used by SIRIUS in the CIC-like file format [8]. These temperatures are then used by SIRIUS to calculate the emitted black-body radiation for every material with its location on the geometry (with the emissivity spectra too). In order to obtain the satellite signature in the LWIR band, all the radiative contributions of the scene are then propagated with SIRIUS to a modeled camera to simulate the detected image.

2.3. Light curve calculation

Light curves describe the temporal evolution of the total flux reflected and emitted by the target object integrated on the instrument field-of-view. We used SIRIUS to calculate the light curves for ENVISAT under conditions identical to those of the observations carried out in 2016 at Graz [21]. The calculation of a light curve with SIRIUS requires a description of the scenario (date, start and end of observation by the telescope, time step, spectral band, possibly meteorological data), description of the satellite (geometry, materials, optical and thermal properties of the materials), the calculation at each time of the satellite's position in the J2000 reference frame using the orbit parameters contained in the TLE file. The ENVISAT geometric model was generated from public data. It consists of a solar panel and a bus equipped with various Earth observation instruments. The solar panel and the parts covered with MLI represent a large portion of the satellite's surface area, so we considered only three categories of material (as done for the thermal model) not to complicate the simulation (solar cells, MLI, and the other parts, mainly the radiators and SAR antenna). The optical properties considered here are typical values taken from the literature [6]. We used the results of [21, 20] to estimate the attitude of ENVISAT.

3. RESULTS: LIGHT CURVES IN VIS/LWIR BANDS

We simulated light curves in the visible and LWIR bands of ENVISAT considering as the observation point the Graz observatory as in [21, 20] in order to model under the same conditions of what is traditionally the main source of tracking of ENVISAT in recent years after the end of its mission. We thus simulated the passage of ENVISAT over Graz back to year 2016. Unfortunately, we could not directly compare our calculated (solar) light curves with the ones measured in [21, 20], since in their case they measured active light curves as the main output of the powerful laser ranging technique. Nevertheless, a direct comparison to the SAR images of [21] can be done (see Fig.(2)). By making use of the attitude estimation of ENVISAT obtained in these studies [21, 20], we constrained the orientation of the satellite in our model and calculated the light curves. We also refer to a previous work for a comparison of light curves in the visible calculated with SIRIUS and compared with ground telescope measurements [6]. In particular, here we focused on the part of the orbit when ENVISAT is coming out from the Earth shadow (see Fig.(1) for the scenario representation). The shadow phase is defined by the portion of the visible light curve which has zero value. From Fig.(3) we see that LWIR light curves allow to track the satellite when it is not directly lighted up by the Sun. Moreover, an estimation of the attitude of the satellite can be maintained even in the shadow phase, thus allowing to exploit a much greater amount of data. Interestingly, we note that the strong specular peaks in the visible are irregu-

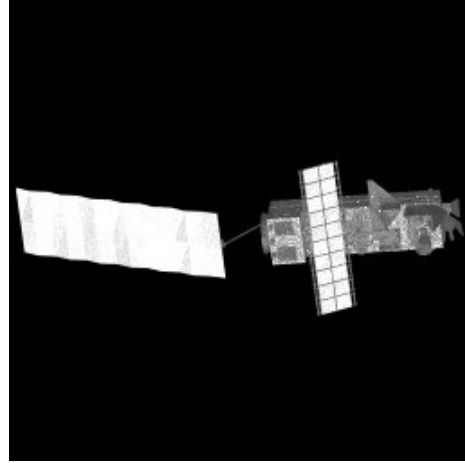


Figure 2. Simulated LWIR image of ENVISAT as it would be seen by the Graz observatory on the day 2016-09-21T20:33:00.

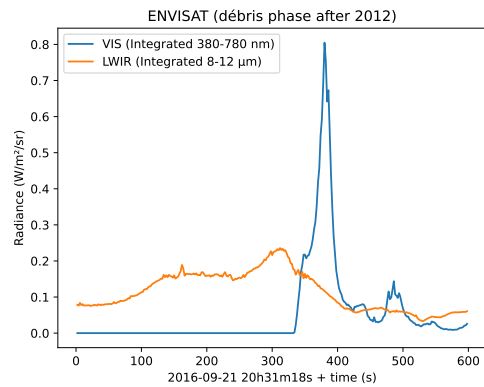


Figure 3. Simulated visible and LWIR light curves of ENVISAT as seen by the Graz observatory in 2016. The zero value part of the visible light curve defines the time interval of the shadow phase (i.e. the satellite lies in the Earth shadow).

lar in time depending strongly on the optical properties and orientation of the objects on the surface of the satellite bus. This feature seems to be unfavorable to reach a good inversion of the light curve to reconstruct the attitude of the satellite over time. On the contrary, LWIR light curves exhibit a low frequency changing behavior in time, thus being more suitable for inversion. We note that in our simulations the amplitude of LWIR light curves is higher when the hot parts of the satellite (the solar panel) are oriented toward the observing telescope (and just spinning around a tilted nadir axis). In the final part of the simulated light curve, the satellite is oriented toward the observer in a way that the solar panel is not directly visible, thus giving a LWIR light curve which is lower in amplitude. Interestingly, the main part of the satellite thermal IR signature comes from the solar panel. Finally, the well known drawback of the thermal infrared detection of space objects from ground telescopes, is the difficulty to extract sufficient signal from the dominating

background radiation coming from the surrounding environment. Notably, recent experimental advances seem to be very promising to make it possible [30, 26]. To conclude, we note that the disturbing effect of the environmental thermal background was not considered in our simulations, thus additional studies need to be done in order to characterize the impact of it on this kind of observations in terms of signal-to-noise ratio.

4. CONCLUSIONS

We demonstrated the new capability of SIRIUS to calculate the thermal infrared signature of a satellite. This is the result of the coupling of the main rendering engine SIRIUS with a satellite thermal model based on COMSOL allowing to evaluate surface temperature of complex geometries in space-like scenarios. In particular, we discussed our findings in term of light curves corresponding to low resolution ground-based telescopes. We found that LWIR light curves do not exhibit sharp peaks over time and depend on the orientation of the bus and the solar panels of the satellite being both influenced by the Sun direct radiation and the Earth emission. Moreover, thermal IR light curves are less influenced by the surface BRDF of the satellite. On the contrary, the main contribution of light curve in the visible comes from very strong specular reflection peaks making them more sensitive to the actual orientation of the objects on the surface of the satellite (and on their optical properties, e.g. the BRDF) rather than the 3D attitude of the satellite itself. All these findings will be exploited in future in order to define a new approach for satellite attitude inversion from ground-based telescope detection.

ACKNOWLEDGMENTS

We thank the PROVIDENCE team at ONERA for valuable discussions and references.

REFERENCES

- Alcayde, V., et al., (2021). Thermal control of a spacecraft: Backward-implicit scheme programming and coating materials analysis, *Advances in Space Research*, **68** (4), 1975-1988.
- Astropy Python Module. www.astropy.org.
- Beltramo-Martin O., et al., (2024). Review of PSF reconstruction methods and application to post-processing, *Adaptive Optics Systems VII*, **11448**, 22–36, SPIE.
- Boushon, K. E. (2018). Thermal analysis and control of small satellites in low Earth orbit. Missouri University of Science and Technology.
- Cognion R.L., (2013). Observations and modeling of GEO satellites at large phase angles, *AMOS proceedings*.
- Coiro E., Tricoli U., Margall F., et al., (2024). Hyperspectral optical modeling of resident space objects at high spatial resolution, *Algorithms, Technologies, and Applications for Multispectral and Hyperspectral Imaging XXX*, SPIE, 70-78.
- <https://www.comsol.com/model/spacecraft-thermal-analysis-109811>
- <https://www.connectbycnes.fr/en/simu-cic>
- de la Villegeorges T., et al., (2024). Towards an All-Orbit Optical Data Service Provisioning Based on ArianeGroup Helix System, *Advanced Maui Optical and Space Surveillance (AMOS) Technologies Conference*, 81.
- Endo T, et al., (2023). Simulating the Photometric Light Curve of Artificial Satellites in GEO used with a Ray-Tracing. In *Proceedings of the Advanced Maui Optical and Space Surveillance (AMOS) Technologies Conference 2023 Sep* (p. 94).
- www.esa.int/Enabling_Support/Operations/Envisat
- www.esatan-tms.com.
- Finckenor M.M., and Dooling D., (1999). Multilayer insulation material guidelines (No. M-925).
- Frei, Walter. “Calculer des chargements thermiques en orbite avec COMSOL Multiphysics®.” COMSOL, 23 Nov. 2022, www.comsol.fr/blogs/computing-orbital-heat-loads-with-comsol-multiphysics.
- Hagerty S., Ansari K., (2019). An innovative near-real-time approach to space situational awareness (ssa) data simulation, *In 35th Space Symposium, Technical Track*.
- Hejduk M. D., (2011). Specular and diffuse components in spherical satellite photometric modeling, *Proceedings of the Advanced Maui Optical and Space Surveillance Technologies Conference*, Maui Economic Development Board.
- Hora J. L., Siraj A., Mommert M., et al., (2018). Infrared light curves of near-Earth objects, *The Astrophysical Journal Supplement Series*, vol. **238**(2), 22.
- Hoarau R., (2019). Rendu interactif d’image hyper spectrale par illumination globale pour la prédiction de la signature infrarouge d’aéronefs, *PhD thesis*, Aix-Marseille Université.
- Hoarau R., Coiro E., Thon S., and Raffin R., (2018). Interactive hyper spectral image rendering on gpu, *Journal of Virtual Reality and Broadcasting*, **15**(4).
- Kucharski D., et al., (2014). Attitude and spin period of space debris envisat measured by satellite laser ranging, *IEEE Transactions on Geoscience and Remote Sensing*, **52**(12), 7651-7.
- Lips T., et al., (2017). Debris Attitude Motion Measurements and Modeling-Observation vs. Simulation. *Advanced Maui Optical and Space Surveillance (AMOS) Technologies Conference*.
- Labarre L., et al., (2011). Matisse-v2.0: new functionalities and comparison with modis satellite images, *Infrared Imaging Systems: Design, Analysis, Modeling, and Testing XXII*, **8014**, 80140Z, International Society for Optics and Photonics.

23. <https://www.maxar.com/>
24. Lawler S.M., Boley A.C., Rein H., (2021). Visibility predictions for near-future satellite megaconstellations: latitudes near 50 will experience the worst light pollution, *The Astronomical Journal*, **163**(1):21.
25. Nunes M., et al., (2022). Hyperspectral Thermal Imaging CubeSat for SSA applications, *23rd Advanced Maui Optical and Space Surveillance Technologies Conference (AMOS)*, Maui, Hawaii.
26. Pearce E.C., et al., (2021). Rapid Discrimination of Resident Space Objects Using Near-Infrared photometry, *AMOS proceedings*.
27. Petit C., et al., (2020). LEO satellite imaging with adaptive optics and marginalized blind deconvolution, *21st AMOS Advanced Maui Optical and Space Surveillance Technologies Conference*.
28. Piergentili F., et al., (2020). LEO object's light-curve acquisition system and their inversion for attitude reconstruction, *Aerospace*, **8**(1),4.
29. Pradhan B., Hickson P., Surdej J., (2019). Serendipitous detection and size estimation of space debris using a survey zenith-pointing telescope, *Acta Astronautica*, **164**,77-83.
30. Rashman M.F., et al., (2019). Uncooled microbolometer arrays for ground-based astronomy. *Monthly Notices of the Royal Astronomical Society*, **492**(1), 480-7.
31. Tricoli U., Margall F., Hofbauer F., and Coiro E., (2024). Modeling the optical signature of a satellite, *OPTRO24 Proceedings*.
32. Velez-Reyes M., Erives H., Najera A., et al., (2022). Understanding non-resolved space object signatures for space domain awareness, *Advanced Maui Optical and Space Surveillance Technologies (AMOS) Conference*.
33. Wang H., et al., (2012). Modeling and validation of photometric characteristics of space targets oriented to space-based observation, *Applied Optics*, **51**(32), 7810-9.
34. Wang Y., et al., (2018). Apparent magnitude calculation method for complex shaped space objects, *Advances in Space Research*, **62**(11), 2988-97.
35. <http://www.spacematdb.com/spacemat/m-datasearch.php?name=Dunmore%20DE320>
36. <https://pypi.org/project/sgp4/>